Nanoscale

Accepted Manuscript

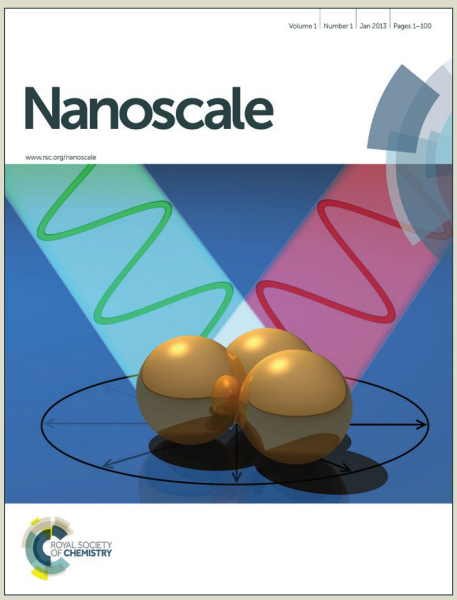

ROYAL SOCIETY OF CHEMISTRY

www.rsc.org/nanoscale

Highly sensitive detection of DNA methylation level by using quantum dots-based FRET method

Yunfei Ma [a,b], Honglian Zhang [b], Fangming Liu [b,], Zhenhua Wu [b], Shaohua Lu[c], Qinhui Jin [b], Jianlong Zhao [b], Xinhua Zhong [a*], Hongju Mao [b*]

[a]*Institute of Applied Chemistry, East China University of Science and Technology, Shanghai, 200237, PR China*

[b]*State Key Laboratory of Transducer Technology, Shanghai Institute of Microsystem and Information Technology, Chinese Academy of Science, Shanghai, 200050, China.*

[c]*Department of Pathology, Zhongshan Hospital, Fudan University, Shanghai, 200032, China.*

***Corresponding Authors:**

Hongju Mao, E-mail: hjmao@mail.sim.ac.cn

Tel: +86-21-62511070-8707; Fax: +86-21-62511070-8714

Xinhua Zhong, E-mail: zhongxh@ecust.edu.cn

Tel: +86 21 6425 0281; Fax: +86 21 6425 0281

Abstract

DNA methylation is the most frequently studied epigenetic modification that is strongly involved in genomic stability and cellular plasticity. Aberrant changes in DNA methylation status are ubiquitous in human cancer and the detection of these changes can be informative for cancer diagnosis. Herein, we reported a facile quantum dots-based (QDs-based) fluorescence resonance energy transfer (FRET) technique for the detection of DNA methylation. The method relies on methylation-sensitive restriction enzymes for the differential digestion of genomic DNA based on its methylation status. Digested DNA is then subjected to PCR amplification for the incorporation of Alexa Fluor-647 (A647) fluorophores. DNA methylation level can be detected qualitatively through gel analysis and quantitatively by the singal amplification from QDs to A647 during FRET. Futhermore, the methylation levels of three tumor suppressor genes, PCDHGB6, HOXA9 and RASSF1A, in 20 lung adenocarcinoma and 20 corresponding adjacent nontumorous tissues (NT) samples were operated to verify the feasibility of the QDs-based FRET method and high sensitivity for cancer detection (up to 90%) was achieved. Our QDs-based FRET method is a convenient, continuous and high-throughput method, being expected to be an alternative for detecting DNA methylation as biomarkers for certain human cancer.

Keywords: DNA methylation, Quantum dots, FRET, PCR amplification, Quantitative analysis

1. Introduction

DNA methylation is an important epigenetic modification that is strongly involved in the physiological control of genome expression.[1] DNA methylation does not alter the primary genomic DNA sequence, instead, it adds a methyl (CH_3) group at the fifth carbon position of a cytosine within a cytosine-guanine (CpG) dinucleotide.[2] CpG dinucleotides are generally underrepresented at the genomic scale, however, high density of CpG dinucleotides (termed CpG islands) has been reported in the promoter regions of approximately 50 % of all genes.[3] In normal cells, promoter-associated CpG islands are generally unmethylated or lowly methylated. In contrast, DNA methylation patterns are largely modified regardless of tissue of origin in cancer cells, which allows for the identification of cancer cells from normal tissues.[4] Moreover, DNA methylation pattern can be further exploited for early cancer diagnosis, cancer-specific gene screening and cancer treatment decision.[5,6]

Due to the increasing significance of DNA methylation in epigenetic modification and its biological application, numerous detection methods have been developed. Summarily, the frequently-used methods for the detection of DNA methylation can be divided into two types: bisulfite-based methods and restriction enzyme-based assays. Bisulfite-based approaches allow for qualitative and quantitative DNA methylation analyses, which also enable the assessment of absolute DNA methylation levels at single-nucleotide resolution.[7] Methylation specific-PCR (MS-PCR) is a sensitive methylation detection method with PCR-assistance,[8] but has been gradually replaced by quantitative MS-PCR (qMS-PCR) because of its non-quantitative nature.[9] Other quantitative approaches have also been developed, such as methylation-sensitive high-resolution melting (MS-HRM),[10] MethyLight,[11] methylation-specific fluorescent amplicon generation (MS-FLAG),[12] methylation-sensitive single-nucleotide primer extension (Ms-SNuPE),[13] combined bisulfite restriction analysis (COBRA)[14] and Pyrosequencing.[15,16] They are all suffered from chemical treatment with sodium bisulfite and achieve the sensitive and quantitative detection of DNA methylation. Some of the disadvantages of bisulfite-based methods that limit their wide application include complications concerning design of dye-labeled DNA probes, the use of radioactive materials,

high cost for the detection, limited read length of DNA and the need for complicated procedure and specialized instruments.

Restriction enzyme-based methods use genomic DNA as starting material and rely on digestion reaction of methylation-sensitive restriction endonucleases prior to PCR amplification.[17,18] Methylation-sensitive restriction enzymes cleave at specific unmethylated recognition sites, leaving methylated sites intact and sensitive to subsequent PCR amplification. Through the analysis of electrophoresis of PCR products, the methylation status of the samples can be determined. This technique allows for simple and sensitive detection, and avoids the poorly controlled efficiency of bisulfite modification, which could generate partial denaturation of DNA duo to the incomplete conversion during treatment.[19] However, the restriction enzyme-based approach does not allow for simultaneous analysis of multiple sites and the methylation detected is not easily quantified.[20]

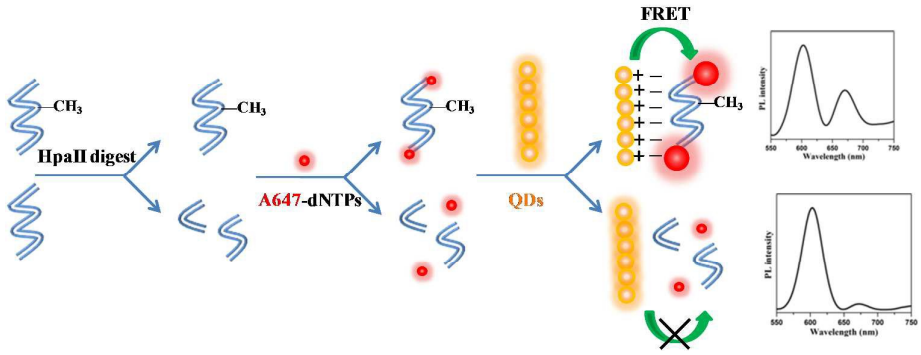

Fig. 1 Schematic illustration of the detection of DNA methylation based on QDs-FRET.

Recently, a new strategy for the optical detection of DNA methylation levels by using cationic conjugated polymers (CCP) has been reported.[21–24] The mechanism of CCP detection process is fluorescence resonance energy transfer (FRET), in which CCP, serving as energy donors, is excited to transfer energy to acceptor fluorophores, leading to significant amplification of fluorescence. In the case of FRET, another highly-fluorescent material, termed as quantum dots (QDs), has been wildly exploited as the FRET donors. Compared with organic molecular fluorophores, QDs have many advantages such as narrow emission

spectra, broad absorption spectra, negligible photobleaching, and high photochemical stability.[25–27] They also possess size-dependent fluorescence emission spectra, which allow for the accommodation of spectral overlap between donors and acceptors by adjusting the particle size during synthesis.[28] Moreover, the large extinction coefficients and wide absorption wavelengths of QDs contribute to excitation of QDs with different emission wavelength by a common excitation source,[29] therefore, making them especially useful in assays that involve multiple FRET pairs. In this study, we present a facile route towards the detection of DNA methylation level via a QDs-based FRET technique. The principle of methylation detection is illustrated in Fig. 1. Brifely, methylated and unmethylated DNAs are firstly identified by the cleavage at specific restriction positions based on the actions of methylation-sensitive restriction enzyme. Then methylated DNA is amplified using conventional PCR, which also simultaneously introduces Alexa Fluor-647 (A647) fluorophore to the PCR product. Through the measurement of generated FRET signal from QDs to A647-labelled DNA due to electrostatic interactions, quantitative detection of DNA methylation level can be finally realized. Moreover, PCDHGB6, HOXA9 and RASSF1A, three of the tumor suppressor genes in lung cancer, were examined using QDs-based FRET techniques to show the feasiblity and high sensitivity for detecting methylation levels of clinical samples. The experimentation simplifies previously available methods by avoiding bisulfite converting, primer labeling, complicated post treatment and sophisticated instruments to achieve expected detection. We expect that the facile method would be a promising tool for the early detection of cancer in research and diagnosis.

2. Experimental section

2.1 Chemicals

oleylamine (OAm, 70%), 1-hexadecylamine (98%), 1-dodecylamine (>99%), oleic acid (99%), 1-octadecene (ODE, >95%) , Cysteamine (Cys) hydrochloride，HEPES and agarose were obtained from Aldrich and used without further purification. HpaII (New England Biolabs), Taq DNA polymerase, deoxynucleotide triphosphates (dNTPs) (including

deoxyadenosine triphosphate (dATP), deoxythymidine triphosphate (dTTP), deoxycytidine triphosphate (dCTP) and deoxyguanosine triphosphate (dGTP)) and shrimp alkaline phosphatase (SAP) were purchased from TaKaRa Biotechnology. Alexa Fluor®647-aha-dUTP and Alexa Fluor®647-aha-dCTP were purchased from Life-technologies.

2.2 Synthesis of amino-CdSe/CdS/ZnS QDs

The starting oil-soluble CdSe/CdS/ZnS QDs were prepared according to previously reported method[30–32] with slight modifition and the detailed procedure is available in Electronic Supplementary Information (ESI). Amino-CdSe/CdS/ZnS QDs were synthesized with Cys by a thiol exchange method.[33] Briefly, 100 mg of Cys (dissolved in 5 ml water) were added dropwise into the oil-soluble QDs in chloroform (10^{-6} M, 20.0 mL) with the help of sonication. The system was not terminated until the layer of chloroform is clear. The colorless organic phase was then discarded. Finally, the aqueous phase containing the QDs was collected and subjected to centrifugation purification using acetone.

2.3 Preparation of tissue and DNA samples

In this study, 40 lung adenocarcinoma cancer and adjacent nontumorous tissues (NT) samples were obtained from 20 patients who underwent primary surgical resection of lung adenocarcinoma in 2014 at Shanghai Zhongshan Hospital. Human samples were obtained with informed consent. The pathological status were appraised by an experienced pathologist. The research was approved by the Institutional Review Board of Shanghai Zhongshan Hospital, China.

Genomic DNA was isolated and extracted from the frozen tissue samples using a AllPrep DNA/RNA Mini Kit (50) (QIAGEN) following the instructions and quantified using a ND-1000 (NanoDrop). Then the genomic DNA was treated with methylation-sensitive restriction enzyme HpaII. Briefly, 100 ng of extracted DNA, 10 units of HpaII, 1 × NEBuffer I and deionized water were mixed in a tube. For the control sample, 100 ng of extracted DNA was subjected to non-HpaII treatment with procedure similar to the digest method mentioned, except for the addition of HpaII. Both reaction systems were incubated at 37 °C overnight,

followed by heat inactivation of HpaII at 85 °C for 15 min. The treated DNA samples were then used for PCR amplification.

2.4 Gene selection and primer design

For this study, three genes, PCDHGB6, HOXA9 and RASSF1A, were selected to determine the methylation levels of their promoters, which could serve as the promising epigenetic markers for lung cancer. All the genes cover at least two CCGG sites and the primer sequences are listed as follows (Table 1).

gene	forward primer (5'–3')	reverse primer (5'–3')	product size (bp)	Number of 5'CCGG3' site
PCDHGB6	GATGTACACCTGCATTTTCG	CGTTCGCTCGGGTTCTCGCT	358	4
HOXA9	CCAACGGGTGAGAATAAAC	AAAAACTACAAGTGGCATGA	348	4
RASSF1A	AAGATCACGGTCCAGCCTC	CTTCGTCCCCTCCTCACAC	307	3

Table 1 Sequences of primers used for amplifying the promoter regions of lung cancer-related genes.

2.5 Detection of methylation level

Methylation levels of the selected genes were detected using the QDs-based FRET method. The treated DNA samples were amplified by one-round PCR. The 20 μL PCR system mixture contained the following: 10 ng DNA samples, primers (0.25 μM each), 1 × dNTPs/A647-dNTPs mix (16 μM dATP, 16 μM dGTP, 14 μM dCTP, 14 μM dTTP, 2 μM A647-dCTP, and 2 μM A647-dUTP), 1 unit Taq polymerase, 1×Taq buffer, and 0.5 mM $MgCl_2$. The reaction was carried out under the conditions listed as follow: 95 °C for 10 min, followed by 40 cycles of 95 °C for 10 s, 55 °C for 10 s, and 72 °C for 30 s, and a final extension step at 72 °C for 10 min. After PCR ampilfication, 5 μL of each sample was loaded in 2% agarose gel in Tris-acetate-ethylenediamine tetraacetic acid (TAE, 0.1×) buffer and ran at 6 V cm^{-1} to observe their imaging with a Gel documentation system. To degrade the excess dNTPs and A647-dNTPs, 1.5 units of shrimp alkaline phosphatase (SAP) (TaKaRa) and 1.8 μL of 10× SAP buffer were mixed with 15 μL PCR products, followed by incubation at 37 °C

for 30 min and heat inactivation of the enzyme at 65 °C for 20 min. After SAP digest, 1 μL of obtained amino-QDs (5 μM) was first diluted in 180 μL HEPES buffer (25 mM, pH 7.0), and then mixed with digested DNA samples in a 96-well plate. Finally, fluorescence measurements were collected using a microwell plate reader (Horiba fluoromax-4 spectrofluorimeter) in order to detecte the degree of FRET reaction after the mixure was incubated at 37 °C for 60 min. To verify the methylation level results obtained from the QDs-based FRET method, pyrosequencing method was conducted using portion of the samples. In brief, 2 μg of tissue samples were converted using an Epitect Bisulfite kit (QIAGEN) following the manufacturer's instructions. Then 2 μL of bisulfate-treated DNA sample was amplified by conventional PCR using premix Taq DNA ploymerase (Takara) in a 30-μL reaction volume. The PCR products were treated in a 96-well plate according to the manufacturer's instructions for pyrosequencing, and were finally loaded into the PyroMark Q96 ID system (QIAGEN) for detection of methylation levels. The primer sequences used for amplifying the promoter regions in pyrosequencing experiment are listed in Table S1.

2.6 Characterization

UV-vis and photoluminescence (PL) spectra were obtained by a Shimadzu UV-2450 UV-vis spectrophotometer and a Horiba fluoromax-4 spectrofluorimeter, respectively. DNA concentration was quantified using a NanoDrop ND-1000. Digital images from gel electrophoresis experiment were captured with the AlphaImager IS-2200 (Alpha Innotech). PCR reacations were carried out on Takala Gradient PCR equipment. The pyrosequencing experiment was performed by PyroMark Q96 ID system (QIAGEN).

3. Results and discussion

3.1 Spectral properties of amino-QDs and A647

The detection of methylation level relies on FRET, with water-soluble amino-CdSe/CdS/ZnS QDs[30–33] acting as the energy donor and A647-labeled DNA as the acceptor. The spectral characteristics of donor and acceptor are studied, as they are crucial to the FRET process. Fig. 2 shows the absorption and emission spectra of the obtained amino-QDs and A647

fluorophore. The QDs emission spectrum shows a maximum wavelength at 600 nm with a narrow full width at half-maximum (FWHM) of about 40 nm, which is partially overlapped with the absorption spectrum of A647 fluorophore. The selection of such sized QDs combined with A647 as an energy-transfer pair also permits minimal spectral cross-talk between donor and acceptor emissions. The broad absorption spectrum of QDs contributes to flexibility in choosing a suitable excitation wavelength to excite the QDs and allows FRET-based target detection with low background. In the case of QDs-A647 pair, sample excitation can be achieved at 450–520 nm, which is near the minimum of the absorption spectrum of A647, thereby nearly eliminating direct acceptor excitation. The as prepared QDs also exhibit high photoluminescence (PL) efficiency and the quantum yield was calculated as 34% by the integrated emission of the QD samples in solution compared with that of rhodamine 6G (PL QYs, 95%) in ethanol under identical optical density.[34]

Based on the FRET pair, we further estimate a Förster distance R_0 (a distance showing 50% energy transfer efficiency)[35] of ~6.91 nm (see calculations in ESI, Data. S1) between QDs and A647, which is the prerequisite of energy transfer. The conjugation of QDs and A647 in our study relies on electrostatic interactions, in which the positively charged amino-QDs forms a complex with negatively charged A647-labeled DNA and therefore brings the A647 fluorophores in close proximity to the QDs. The donor–acceptor separation drived from electrostatic interactions is considered much shorter than Förster distance R_0 and the FRET efficiency exceeding 50% is expected.[36] It is also worth noting that the electrostatic interaction is a more labour-saving and cost-saving way to connect FRET pairs than conventional covalent linking.[36]

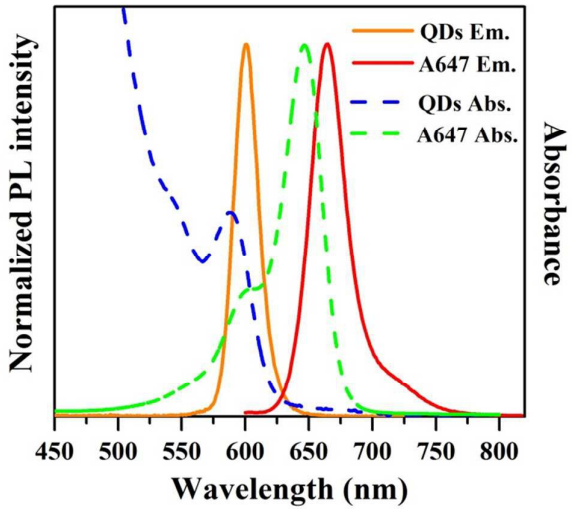

Fig. 2 Normalized UV–vis absorption (abs) and fluorescence emission (em) spectra of A647 and amino-QDs.

3.2 Principle of QDs-based methylation detection approach

The detection of DNA methylation is on the basis of the use of methylation-sensitive restriction enzymes, which can recognize specific restriction positions and are sensitive to nucleoside methylation. In this study, we subjected DNA samples to restriction digestion by HpaII, an enzyme that cleaves at unmethylated 5'-CCGG-3' sites. The mechanism of QDs-based methylation detection is illustrated in Fig. 1. Firstly, genomic DNA is treated with HpaII, in which all unmethylated recognition sites are cleaved, while leaving methylated DNA intact. Next, DNA is amplified using conventional PCR, accompanied by the incorporation of A647-dNTPs. The methylated DNA templates in sample are amplified upon HpaII treatment as it was insensitive to the cleavage by HpaII and hence retains an intact DNA strand, while PCR amplification does not occur for unmethylated DNA. Finally, the dye-labeled PCR products are mixed with QDs solution to generate FRET signal due to the electrostatic interactions between positively charged QDs and negatively charged DNA. The FRET signal is determined by the A647 fluorophores incorporated in DNA, hence methylated DNA templates can generate strong FRET signal. For unmethylated DNA, A647 fluorophores disperse randomly in the system without being labeled in DNA and Förster distance R_0 discussed above will not be satisfied, leading to the failure of FRET signal. In other words,

the FRET signal is proportional to the amount of dye-labeled DNA. Based on the above principle, parameter E is defined to measure methylation level with a subtracted background, where FRET $ratio_{HpaII}$ refers to the ratio of emission intensities of A647 to QDs (I_{670} nm/I_{600} nm) for the HpaII-treated sample, FRET $ratio_{blank}$, serving as the background, refers to the FRET ratio for the negative non-template control. In the case of FRET $ratio_{non\text{-}HpaII}$, it represents the FRET ratio for the HpaII-untreated sample. Both methylated and unmethylated DNAs are amplified to incorporate A647-dNTPs in HpaII-untreated samples. Thus, the addition of QDs can result in highly efficient FRET signals due to the contribution of the whole genomic DNAs.

$$E = \frac{\text{FRET ratio}_{HpaII} - \text{FRET ratio}_{blank}}{\text{FRET ratio}_{non\text{-}HpaII} - \text{FRET ratio}_{blank}}$$

3.3 Influence of experimental variables

In this work, we examined gene methylation in cases of lung adenocarcinoma. Three lung cancer-related genes were selected based on published literature; these include PCDHGB6 (protocadherin gamma subfamily B6), HOXA9 (homeobox A9) and RASSF1A (RAS association domain factor 1A).[37–39] Since PCR conditions are crucial to PCR-related protocols due to the potentials for false positives or negatives, we carefully optimized the PCR condition to ensure the sensitivity and specificity of PCR experiments performed in this study. In our study, we conducted only one round of PCR instead of adopting the nested PCR protocol reported in Wang et al.[22–24] The nested approach requires setting up more than one PCR reaction, and the multistep process could lead to low experimental repeatability and potential false-positive results in amplification. As for the addition of A647-labeled nucleotide triphosphates, A647-dUTP and A647-dCTP were chosen to be incorporated simultaneously, which is more efficient than using them separately. The simultaneous addition could also eliminate bias arouse from differences in GC fractions since double-stranded DNA has an identical (dT+dC) value.[23] It should be noted that A647-dNTPs, instead of dye-labeled primers reported by other groups,[11] are introduced in our protocol,

which not only simplifies the experimental design, but also reduces the cost of the experiment. In our experiment, the dNTPs concentration was kept as low as 16 μM and the fraction of dye-labeled dNTPs was set as 1/8 to ensure sufficient incorporation. It should be noted that the fraction of dye-labeled dNTPs used is crucial since incorporation would be too difficult to monitor if fraction used was too low. It is also possible that, extension rate during PCR amplification would be restricted if fraction used was too high. The control experiments were also performed as the background signal, and water instead of genomic DNA can commonly serve as a negative control. Notably, the PCR products should be avoided to form hairpins, dimers, and cross-dimers. If so, it should elevate the annealing temperature or redesign the primers to guarantee high specificity.

3.4 Qualitative analysis of DNA methylation level

Gel electrophoresis is inevitable to be studied to decide whether HpaII truly reflects the methylation status of the target genes. As shown in Fig. 3, electrophoresis analysis of PCR products of the three genes exhibits high specificity of PCR amplification. The sizes of PCR products are consistent with the expected lengths of 358 bp for PCDHGB6, 348 bp for the HOXA9 and 307 bp for RASSF1A. The primers designed for PCR are listed in Table 1 in Experimental Section. For each gene, the gel image of HpaII-treated, HpaII-untreated and negative PCR products of NT and cancer tissues are listed respectively. From Fig. 3, HpaII-untreated PCR products show high specificity and high intensities due to the contribution of the amplification of both methylated and unmethylated DNAs, while no images are found for the negative non-template control. However, PCR products of HpaII-treated samples exhibit various levels of intensities due to the cleavage of unmethylated parts in samples. Generally, low degree of intensity was usually observed with PCR products from NT tissues, while moderate and high intensity was exhibited by DNA from most cancer tissues. The phenomenon indicates that there are differences in the proportion of methylated and unmethylated DNA between HpaII-treated NT tissues and cancer tissues. Therefore, we concluded that the methylation level of DNA samples can be qualitatively interpreted from

gel electrophoresis of restriction enzyme treated PCR products.

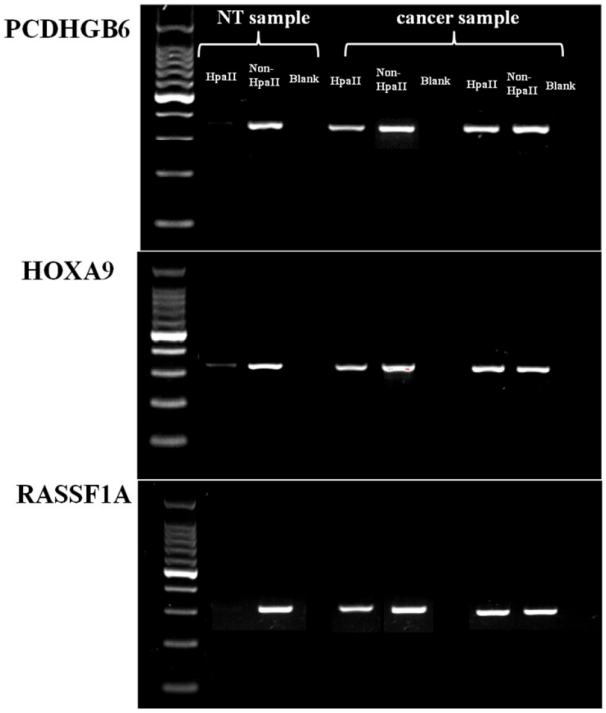

Fig. 3 Gel analysis of PCR products of PCDHGB6, HOXA9 and RASSF1A genes in 2% (wt/vol) agarose gel. For each gene, the left lane is for the HpaII-PCR products, and the middle lane is for the non-HpaII PCR products, and the right lane is for the blank PCR products. Low image intensities of HpaII-treated samples were usually observed with PCR products from NT tissues, while higher degrees were observed with PCR products from most cancer tissues.

3.5 Quantitative analysis of DNA methylation level

After gel analysis, PCR products were treated with alkaline phosphatase to degrade the excess dNTPs and A647-dNTPs, and then mixed with amino-QDs solution to conduct fluorescence analysis. The electrostatic interactions of positively charged amion-QDs and negatively charged DNA brought the A647 fluorophores in close proximity to the QDs. When QDs were excited at 500 nm, they efficiently transferred energy to the fluorophores via FRET, producing an amplified A647 fluorescence signal that could be used to detect the presence of PCR products. In addition, variations in the amount of dye-labeled DNA PCR products would

result in different A647 to QDs emission fluorescence ratio, thereby allowed for the quantitative determination of DNA methylation level based on FRET fluorescence signal. Spectra for the different fluorescence signals from FRET for the PCDHGB6 gene are shown in Fig. 4a, b, c. Low FRET ratio (I_{670} nm/I_{600} nm) was observed in the negative non-template control, which could be attributed to the failure of generating FRET from QDs to A647 without dye-labeled DNA amplification. In contrast, high FRET ratio was demonstrated by the HpaII-untreated PCR products, which could be contributed to the amplification of the whole genomic DNAs in samples. The vast negatively charged dye-labeled DNA formed a complex with positively charged amino-QDs and therefore led to an obvious optical amplification of A647 fluorophore. For HpaII-treated samples, efficiencies of FRET varied depending on the amounts of generated A647-labeled DNA products. Generally, high amounts of PCR products generate high FRET ratio, and vice versa. Corresponding schematic illustrations of the different levels of FRET ratio observed are shown in Fig. 4d, e, f. Parameter E illustrated above was defined to quantitatively compare the different degrees of FRET, and could be used to represent DNA methylation levels. In general, low E was observed in PCR products from NT tissues, while moderate and high E were found in PCR products from most cancer tissues. It should be noted that the quantitative analysis of methylation level is accomplished by frequently-used fluorescence spectrometer, replacing the expensive specialized quantitative real-time PCR machines or sequencing machine used in previously available methods. Furthermore, to realize the methylation detection of a large number of clinical samples simultaneously, the high-throughput method is necessary.[16, 40-41] In the study, the high-throughput detection of FRET signal is realized by using a microwell plate reader.

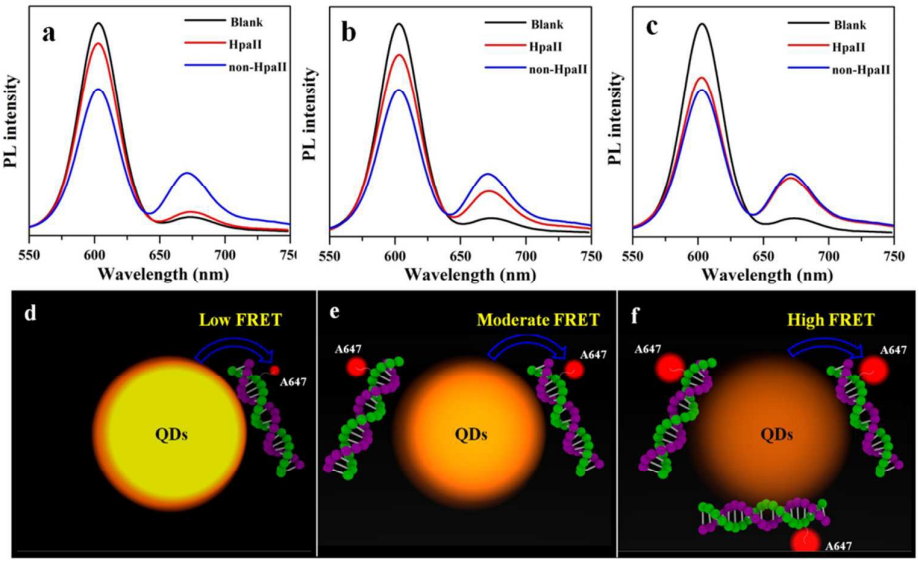

Fig. 4 Fluorescence spectra of different methylation levels, including low (a), moderate (b), and high (c), in which QDs were excited at 500 nm. Corresponding schematic illustrations of low FRET level (d), moderate FRET level (e), and high FRET level (f) from in HpaII-treated samples.

DNA methylation based biomarkers are in high demand as they provide a non-invasive way to detect tumors of different types. In this study, PCDHGB6, HOXA9 and RASSF1A, three tumor suppressor genes, were investigated and identified as methylated in lung cancer tissues. PCDHGB6 is a member of the protocadherin gamma gene cluster, which has an immunoglobulin-like organization, and it has been proposed that a novel mechanism may be involved in its regulation and expression.[37] HOXA9 is part of the homeobox A cluster on chromosome 7 and encodes a DNA-binding transcription factor, which may be involved in regulating gene expression, morphogenesis, and differentiation.[38] RASSF1A is a tumor suppressor gene that can induce apoptosis, regulate proliferation, and stabilize microtubules.[39]

To investigate the potential of DNA methylation levels of the three selected genes as biomarkers for cancer diagnosis, 20 lung cancer samples and 20 corresponding NT samples were tested to verify the feasibility of using QDs-based FRET to measure DNA methylation. Based on the calculation of equation E, the methylation levels of PCDHGB6, HOXA9 and RASSF1A genes are presented in Fig. 5. Portions of the samples were also subjected to

pyrosequencing to validate the methylation levels calculated from the QDs-based FRET method. Pyrosequencing is a highly reliable, quantitative and real-time sequencing method, based on the luminometric detection of pyrophosphate (PP_i) release upon nucleotide incorporation by an enzymatic cascade, and allows for allele frequency determination for single nucleotide polymorphisms, and is gradually considered as the gold standard for methylation detection.[15–16] However, the wide application of pyrosequencing is still limited by the skilled operation and specialized instrument. In addition, only short-length DNA templates can be detected due to the thermal instability of the enzymes used in sequencing. Following the principle of pyrosequencing method, we converted the genomic DNA by bisulfite treatment and amplified with PCR primers for the three genes shown in Table S1. During pyrosequencing reaction, each gene should cover several methylation variable positions in the CpG island, among which ten positions for PCDHGB6, six for HOXA9 and three for RASSF1A were analyzed. Fig. S1 shows an example of the methylation analysis of the RASSF1A gene in one pair of NT and cancer samples by pyrosequencing. The y-axis represents signal intensity while the x-axis shows the nucleotide dispensation order. All positions can be analyzed simultaneously and the percentages of methylation at individual CpG positions are shown above the respective positions. In order to compare the result with the methylation levels measured by QDs-based method, we determined an average of the methylation values at all positions in pyrosequencing as the single methylation levels of samples in the study. For example, the methylation levels can be averaged by three values in variable positions in Fig. S1, and the quantitative value is 24.67% for NT sample, and 68.34% for cancer sample. The comparisons of results on parts of NT and cancer samples from the QDs-based FRET and the pyrosequencing method are shown in Table S2. The methylation levels detected by the QDs-based FRET method are not absolutely accurate with some measurements being higher than those indicated from the corresponding pyrosequencing results, which may be due to the incomplete digestion of DNA samples by restriction enzyme HpaII and the conditions of PCR amplification, However, the general trend in the difference between cancer samples and NT samples is consistent between the pyrosequencing results and

those from QD-based FRET, demonstrating that QDs-based FRET method is an efficient technique and worth being considered for practical application.

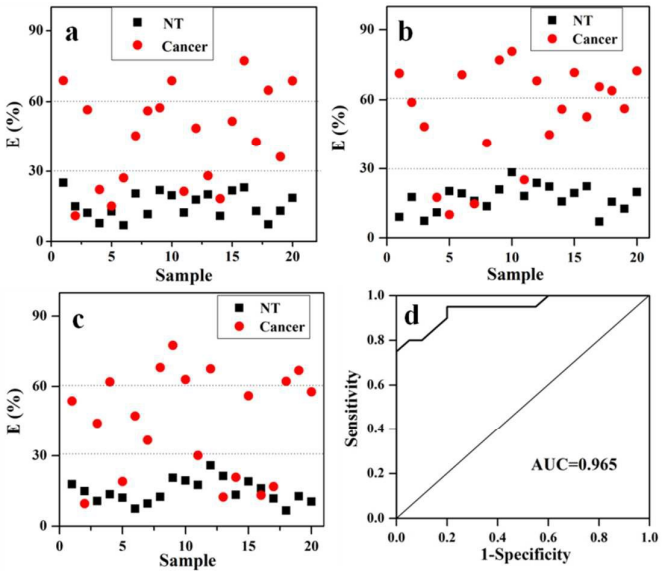

Fig. 5 Methylation levels of PCDHGB6 (a), HOXA9 (b) and RASSF1A (c) in 20 cancer samples and 20 NT samples as measured by the QDs-based FRET technique. (d) ROC curves analysis for using the combination of the three genes of interest for the discrimination of lung adenocarcinoma tissues from NT samples.

From Fig. 5a, b, c, as expected, the averages of methylation levels of PCDHGB6, HOXA9 and RASSF1A in cancer cases are obviously higher than that in the adjacent nontumorous tissues (NT) control. It is worth noting that NT samples were obtained near the lung tumor tissues of patients, and low methylation levels, not non-methylation, still exists in NT samples, which has been verified by pyrosequencing method. With regard to the PCDHGB6 gene, methylation levels in all 20 NT samples are below 30%, while those in 5 out of 20 lung cancer samples are above 60%; 8 out of 20 lung cancer samples are between 30 and 60%; 7 out of 20 cancer samples have methylation levels below 30%. As for the HOXA9 gene, all NT samples are below 30%; 9 out of 20 lung cancer samples are above 60%; 7 out of 20 lung cancer samples are between 30% and 60%; and 4 out of 20 are below 30%. Regarding the RASSF1A gene, the methylation level of all 20 NT samples are below 30%; 7 out of 20 lung cancer samples are above 60%; 6 out of 20 lung cancer samples are between 30% and 60%;

and 7 out of 20 are below 30%. Based on these results, we roughly divided the methylation levels of the three genes into three sections: low methylation level includes those below 30%, moderate methylation level represents those between 30% and 60%, and high methylation level indicates those above 60%. We further evaluated the diagnostic potential of combining results from all three genes using receiver operating characteristic (ROC) curve analysis. As shown in Table 2, the single PCDHGB6 gene, HOXA9 gene and RASSF1A gene show the area under receiver operating characteristic curve (AUC) value of 0.860, 0.867 and 0.820 (all $P<0.001$) in differentiating lung adenocarcinoma from NT samples respectively. When optimum thresholds were selected, the sensitivity of single gene is 65% for PCDHGB6, 80% for HOXA9, and 60% for RASSF1A, the specificity is 100% for PCDHGB6, 95% for HOXA9 and 100% for RASSF1A. Based on the logistic regression model, the combination detection mode of three biomarkers was built. The combination of using all three genes produced an AUC value of 0.965 ($P<0.001$), which is higher than the AUC of each individual gene (ROC curve of the combination of three biomarkers is shown in Fig. 5d). The sensitivity of using all three genes is 90% as acquired from ROC curve analysis, which is higher than the sensitivity of using any of the three genes alone. These results confirm that highly sensitive detection of methylation levels can be achieved by our QDs-based FRET method.

Detection mode	AUC	Sensitivity (%)	Specificity (%)
Single PCDHGB6	0.860	65	100
Single HOXA9	0.867	80	95
Single RASSF1A	0.820	60	100
Combination of three biomarkers	0.965	90	95

Table 2 Sensitivity and specificity of using combination and single biomarker for methylation detection in a total of 40 lung adenocarcinoma and NT tissues.

4. Conclusions

In summary, we took advantage of the QDs-based FRET method to successfully detect

DNA methylation levels in cancer tissues. Using methylation-sensitive restriction endonucleases, methylated and unmethylated DNAs were distinguished, and the levels of methylation were detected qualitatively through gel analysis and quantitatively by the singal amplification from QDs to A647 based on FRET. PCDHGB6, HOXA9 and RASSF1A, three of the tumor suppressor genes in lung cancer, were examined using the aforementioned techniques. The results show that the method we adopted is feasible and highly sensitive to detecting methylation levels (sensitivity is up to 90%). Compared with other methods of DNA methylation detection, ours is not only a convenient, continuous and high-throughput method; it also does not involve skilled operation and specialized instrument. Furthermore, only a small amount of DNA in samples is needed in our method. Different from most fluorescence-based techniques, A647-labeled nucleotide triphosphates, instead of dye-labeled DNA probes, are introduced in our protocol. This switch not only simplifies the experimental design, but also reduces the cost of the experiment. In addition, the methylation-sensitive restriction endonuclease required by our protocol is not restricted to HpaII. Other enzymes such as HhaI (recognizing 5'GCGC3' site)[42] or BstUI (recognizing 5'-CGCG-3')[43] can also perform the same function for other specific genes. Most importantly, the QDs-based FRET method provides a non-invasive option for early cancer detection, diagnosis, prognosis, therapeutic stratification.

Acknowledgements. This work was supported by Grants from the National Basic Research Program of China (973 Program) (No. 2012CB933303), the National Science Foundation of China (No. 61571429, 61401442, 21275153, 61006086, 21175043 and 21301059), Science and Technology Commission of Shanghai Municipality (Grant No. 12441902600), Shanghai Clinical Center/Shanghai Xuhui Central Hospital, Chinese Academic of Sciences (No.BRC2012002).

Notes and references

State Key Laboratory of Transducer Technology, Shanghai Institute of Microsystem and Information

Technology, Chinese Academy of Science, Shanghai, 200050, P.R. China

E-mail: hjmao@mail.sim.ac.cn; Tel: +86-21-62511070-8707 Fax: +86-21-62511070-8714

Shanghai Key Laboratory of Functional Materials Chemistry, Institute of Applied Chemistry, East China University of Science and Technology, Shanghai 200237, China.

Email: zhongxh@ecust.edu.cn; Fax: +86 21 6425 0281

† Electronic Supplementary Information (ESI) available: Synthesis of CdSe/CdS/ZnS core/shell/shell QDs. Sequences of primers used for amplifying the promoter regions in bisulfate-modified DNA. Comparision of detected methylation levels in different gene promoters using the QDs-based FRET method versus bisulfite pyrosequencing. Methylation level of the RASSF1A gene in one pair of NT and cancer samples as indicated by pyrosequencing. Theoretical calculation of the Förster distance R_0.

1 H. Heyn and M. Esteller, *Nat. Rev. Genet.,* 2012, **13***,* 679–692.

2 A. Bird, *Genes Dev.,* 2002, **16**, 6–21.

3 P. A. Jones, *Nat. Rev.,* 2012**, 13***,* 484–492.

4 R. Lister, M. Pelizzola, R. H. Dowen, R. D. Hawkins, G. Hon, J. Tonti-Filippini, J. R. Nery, L. Lee, Z. Ye and Q. M. Ngo, *Nature,* 2009, **462,** 315–322.

5 A. How Kit, H. M. Nielsen and J. Tost, *Biochimie,* 2012, **94**, 2314–2337.

6 L. D. Moore, T. Le and G. Fan, *Neuropsychopharmacology,* 2013, **38,** 23–38.

7 G. Egger, M. Wielscher, W. Pulverer, A. Kriegner and A. Weinhäusel, *Expert Rev. Mol. Diagn*., 2012, **12,** 75–92.

8 J. G. Herman, J. R. Graff, S. Myöhänen, B. D. Nelkin and S. B. Baylin, *P. Natl. Acad. Sci.*, 1996, **93**, 9821–9826.

9 U. Lehmann, F. Länger, H. Feist, S. Glöckner, B. Hasemeier and H. Kreipe, *Am. J. Pathol.,* 2002, **160**, 605–612.

10 T. K. Wojdacz and A. Dobrovic, *Nucleic Acids Res.*, 2007, **35**, e41.

11 C. A. Eads, K. D. Danenberg, K. Kawakami, L. B. Saltz, C. Blake, D. Shibata, P. V. Danenberg and P. W. Laird, *Nucleic Acids Res.*, 2000, **28**, e32.

12 C. Bonanno, E. Shehi, D. Adlerstein and G. M. Makrigiorgos, *Clin. Chem.*, 2007, **53**, 2119–2127.

13 M. L. Gonzalgo and P. A. Jones, *Nucleic Acids Res.*, 1997, **25**, 2529–2531.

14 Z. Xiong and P. W. Laird, *Nucleic Acids Res.*, 1997, **25**, 2532–2534.

15 S. Colella, L. Shen, K. Baggerly, J. Issa and R. Krahe, *Biotechniques*, 2003, **35**, 146-151.

16 J. Tost and I. G. Gut, *Nat. Protoc.*, 2007, **2**, 2265–2275.

17 T. Mikeska, C. Bock, H. Do and A. Dobrovic, *Expert Rev. Mol. Diagn.*, 2012, **12**, 473–487.

18 A. A. Melnikov, R. B. Gartenhaus, A. S. Levenson, N. A. Motchoulskaia and V. V. Levenson, *Nucleic Acids Res.*, 2005, **33**, e93.

19 L. Van De Voorde, R. Speeckaert, D. Van Gestel, M. Bracke, W. De Neve, J. Delanghe and M. Speeckaert, *Muta. Res.*, 2012, **751**, 304–325.

20 M. A. Clarke, N. Wentzensen, L. Mirabello, A. Ghosh, S. Wacholder, A. Harari, A. Lorincz, M. Schiffman and R. D. Burk, *Cancer Epidemiol Biomarkers Prev.*, 2012, **21**, 2125–2137.

21 F. Feng, H. Wang, L. Han and S. Wang, *J. Am. Chem. Soc.*, 2008, **130**, 11338–11343.

22 F. Feng, L. Liu and S. Wang, *Nat. Protoc.*, 2010, **5**, 1255–1264.

23 Q. Yang, Y. Dong, W. Wu, C. Zhu, H. Chong, J. Lu, D. Yu, L. Liu, F. Lv and S. Wang, *Nat. Commun.*, 2012, **3**, 1206–1213.

24 J. Zhang, B. Xing, J. Song, F. Zhang, C. Nie, L. Jiao, L. Liu, F. Lv and S. Wang, *Anal. Chem.*, 2014, **86**, 346–350.

25 X. Wang, X. Lou, Y. Wang, Q. Guo, Z. Fang, X. Zhong, H. Mao, Q. Jin, L. Wu and H. Zhao, *Biosens. Bioelectron*, 2010, **25**, 1934–1940.

26 A. R. Clapp, I. L. Medintz and H. Mattoussi, *ChemPhysChem*, 2006, **7**, 47–57.

27 U. Resch-Genger, M. Grabolle, S. Cavaliere-Jaricot, R. Nitschke and T. Nann, *Nat. Meth.*,

2008, **5**, 763–775.

28 E. R. Goldman, A. R. Clapp, G. P. Anderson, H. T. Uyeda, J. M. Mauro, I. L. Medintz and H. Mattoussi, *Anal. Chem.*, 2004, **76**, 684–688.

29 P. Reiss, M. Protiere and L. Li, *Small*, 2009, **5**, 154–168.

30 J. J. Li, Y. A. Wang, W. Guo, J. C. Keay, T. D. Mishima, M. B. Johnson and X. Peng, *J. Am. Chem. Soc*., 2003, **125**, 12567–12575.

31 R. Xie, U. Kolb, J. Li, T. Basché and A. Mews, *J. Am. Chem. Soc.*, 2005, **127**, 7480–7488.

32 Y. Ma, Y. Li, S. Ma and X. Zhong, *J. Mater. Chem. B*, 2014, **2**, 5043–5051.

33 C. M. Lee, D. Jang, S.-J. Cheong, E.-M. Kim, M.-H. Jeong, S.-H. Kim, D. W. Kim, S. T. Lim, M.-H. Sohn and H.-J. Jeong, *Nanotechnology*, 2010, **21**, 285102.

34 M. D. Regulacio and M. Y. Han, *Acc. Chem. Res*., 2010, **43,** 621–630.

35 E. R. Goldman, I. L. Medintz, J. L. Whitley, A. Hayhurst, A. R. Clapp, H. T. Uyeda, J. R. Deschamps, M. E. Lassman and H. Mattoussi, J. Am. Chem. Soc., 2005, **127**, 6744–6751.

36 G. Jiang, A. S. Susha, A. A. Lutich, F. D. Stefani, J. Feldmann and A. L. Rogach, *ACS nano*, 2009, **3**, 4127–4131.

37 J. Sandoval, J. Mendez-Gonzalez, E. Nadal, G. Chen, F. J. Carmona, S. Sayols, S. Moran, H. Heyn, M. Vizoso and A. Gomez, *J. Clin. Oncol.*, 2013, **31**, 4140–4147.

38 S.-H. Hwang, K. U. Kim, J.-E. Kim, H.-H. Kim, M. K. Lee, C. H. Lee, S.-Y. Lee, T. Oh and S. An, *Clin. Chem. Lab Med.*, 2011, **49**, 699–704.

39 A. Agathanggelou, W. N. Cooper and F. Latif, *Cancer Res.*, 2005, **65**, 3497–3508.

40 S. Li, H. Liu, Y. Deng, L. Lin and N. He, *J. Biomed. Nanotechnol*, 2013, **9**, 1254–1260.

41 S. Li, H. Liu, Y. Jia, X. Mou, Y. Deng, L. Lin and N. He, *J. Biomed. Nanotechnol*, 2013, **9**, 689–698.

42 D. Frumkin, A. Wasserstrom, B. Budowle and A. Davidson, *Forensic Sci. Int. Genet*, 2011, **5**, 517–524.

43 L. F. Cheow, S. R. Quake, W. F. Burkholder and D. M. Messerschmidt, *Nat. Protoc.*, 2015, **10**, 619–631.

Table of Contents (TOC)

Highly sensitive detection of DNA methylation level by using quantum dots-based FRET method

Yunfei Ma [a,b], Honglian Zhang [b], Fangming Liu [b], Zhenhua Wu [b], Shaohua Lu [c], Qinhui Jin [b], Jianlong Zhao [b], Xinhua Zhong [a*], Hongju Mao [b*]

A quantum dots-based FRET method was established for highly sensitive detection of DNA methylation level.